Hyperfine Interact (2006) 170:105–116
DOI 10.1007/s10751-006-9468-1

# Anisotropic contributions to the transferred hyperfine field studied using a field-induced spin-reorientation

**Laura K. Perry · D. H. Ryan · G. Venturini**

Published online: 9 January 2007


**Abstract** We report here a comparison between a field-driven spin-flop ($TbMn_6Sn_{5.46}In_{0.54}$) and a temperature-driven spin reorientation ($TbMn_6Sn_{6-x}Ga_x$) in order to demonstrate that the anisotropic contribution to $B_{hf}$ at the Sn sites can be obtained through the moment reorientation and is independent of the driving force. We show that a complete 90° spin reorientation can be achieved at 300 K in an applied field of 0.57(3) T and that the changes in hyperfine field due to the anisotropic contribution exceed 45% at one of the Sn sites. Quantitative values for the anisotropic constant at the three Sn sites are obtained.

**Key words** field-driven spin-flop · temperature-driven spin reorientation · moment reorientation · anisotropic contribution

## 1 Introduction

As Sn is non-magnetic, any hyperfine field measured at a Sn site in a crystal structure must be transferred to it from surrounding magnetic moments. This transferred hyperfine field has two main contributions [1]: isotropic and anisotropic. The isotropic contribution is due to conduction band polarization, which induces a spin imbalance at the nucleus. This is commonly referred to as the Fermi contact field, and depends only on the magnitude of the neighbouring moments and the symmetry of their magnetic structure. The anisotropic contribution involves the bonding between the

L. K. Perry · D. H. Ryan (✉)
Center for the Physics of Materials, Department of Physics, McGill University,
Rutherford Building, 3600 University Street, H3A 2T8 Montréal, Québec, Canada
e-mail: dhryan@physics.mcgill.ca

L. K. Perry · G. Venturini
Laboratoire de Chimie du Solide Minérale, Université Henri Poincaré Nancy I,
UMR 7555 BP 239, 54506 Vandoeuvre-les-Nancy, France

magnetic ion and the non-magnetic Mössbauer probe, leading to a transferred field which depends not only on the magnitude of the neighbouring moments, but also on the relative orientations of those moments and their connecting bonds. In the tetragonal $CuAl_2$-type $TSn_2$ (T = Mn, Fe) stannides, the isotropic contribution to the transferred hyperfine field at some ($MnSn_2$ [2]) or all ($FeSn_2$ [3]) of the Sn sites cancels, resulting in a transferred hyperfine field that is totally anisotropic. The hexagonal $HfFe_6Ge_6$-type structure of the $RMn_6Sn_{6-x}X_x$ family of compounds does not allow for such a cancellation, and both contributions to $B_{hf}$ are present. In this case, the isotropic and anisotropic contributions cannot be distinguished unless a process is induced which would change only one of them. The spin reorientation process is a pure rotation of the magnetic structure relative to the crystal axes. Since the moments do not change either size or distance from the Sn site, nor does the magnetic symmetry change, the Fermi contact field cannot change under such a rotation. The isotropic contribution can therefore be isolated from the overall transferred hyperfine field at the Sn sites, and the anisotropic contribution can be determined uniquely.

A spin reorientation can be either temperature-induced or field-induced. At room temperature in $HfMn_6Sn_6$, the Mn moments are oriented in the *ab*-plane (the Mn sublattice has planar anisotropy). In $TbMn_6Sn_6$ at room temperature, the Tb and Mn moments lie along the *c*-axis, indicating the Tb sublattice to have uniaxial anisotropy which dominates over the planar anisotropy of the Mn sublattice. As the Tb anisotropy is more strongly temperature dependent, it decreases more rapidly on heating than that of the Mn. At $T_{sr}$ = 330 K [4], the two sublattice anisotropies are equal, and above $T_{sr}$ the planar Mn anisotropy dominates. The switch in dominant anisotropy causes the Tb and Mn moments to undergo a spontaneous reorientation from the *c*-axis to the *ab*-plane (on heating through $T_{sr}$). Alternatively, by applying a sufficient field perpendicular to the moment direction in a single crystal, we can induce a spin-flop to the direction along which the field is applied.

We have previously studied the anisotropic transferred hyperfine fields in $TbMn_6Sn_{6-x}Ga_x$ ($x = 0.2, 0.4, 0.6$ and 0.8) [5] through $^{119}$Sn Mössbauer spectroscopy. This system undergoes a temperature-induced spin reorientation from the *ab*-plane to the *c*-axis on cooling through $T_{sr}$. The temperature at which the spin reorientation occurs was shown to decrease with increasing *x*. $TbMn_6Sn_{5.46}In_{0.54}$ single crystals undergo a spin-flop transition in quite modest fields around room temperature, and the single crystals can be grown as thin platelets suitable for Mössbauer studies. Here, we compare the spin-flop in $TbMn_6Sn_{5.46}In_{0.54}$ single crystals with the temperature-induced spin reorientation in $TbMn_6Sn_{6-x}Ga_x$ in order to demonstrate that the anisotropic contribution to the hyperfine field is independent of the driving force of the reorientation. We confirm that the Tb and Mn moments lie along *c* for $T < T_{sr}$ and use the electric field gradient to show that the spin reorientation in both systems involves a full rotation of the moments by 90°. The anisotropic contribution to $B_{hf}$ is determined through this rotation.

## 2 Experimental methods

The $TbMn_6Sn_{6-x}Ga_x$ ($x = 0.2$, 0.4, 0.6 and 0.8) compounds were prepared by alloying stoichiometric amounts of ternary $TbMn_6Sn_6$ and $TbMn_6Ga_6$ compounds in

an induction furnace [6]. The resulting ingots were sealed under argon in quartz tubes and annealed for 2 weeks at 973 K.

The $TbMn_6Sn_{5.46}In_{0.54}$ single crystals were synthesized using a flux method similar to that previously reported by Clatterbuck et al. [7]. A mixture of $TbMn_6Sn_6$ and indium and tin metal (99.9% pure) with the atomic ratio $TbMn_6Sn_{23}In_{37}$ was compacted into pellets and put into a silica tube with a quartz-wool stopper. The silica tube was sealed under argon (267 mbar) and heated to 1,273 K (at 50 K/h) for 24 h, after which it was cooled to 1,223 K (6 K/h). The sample was then reheated to 1,263 K at the same rate and finally cooled slowly to 873 K in 65 h. The tube was quickly removed from the furnace, inverted and centrifuged manually using a David's sling device. The (Sn,In) flux settled to the bottom of the tube and the hexagonal crystal platelets (∼1–2 mm in diameter and ∼60 $\mu$m thick) remained on the quartz-wool stopper. Some of the platelets were ground and analyzed by x-ray diffraction Guinier patterns with Cu-$K_\alpha$ radiation. Both $TbMn_6Sn_{5.46}In_{0.54}$ and $TbMn_6Sn_{6-x}Ga_x$ are isotypic with the $HfFe_6Ge_6$ structure.

Mössbauer spectra were collected using a 10 mCi $^{119m}SnCaSnO_3$ source and the spectrometer was calibrated with $\alpha$-Fe and a $^{57}Co$ source. Basic magnetic characterization was carried out on a commercial 9 T susceptometer/magnetometer. For the $TbMn_6Sn_{6-x}Ga_x$ samples, the temperature was varied from 12 to 300 K using a vibration-isolated closed-cycle refrigerator. The $TbMn_6Sn_{5.46}In_{0.54}$ sample was made of single crystal platelets with the *c*-axis perpendicular to the plane of the plates. The platelets were assembled in a mosaïc and subject to external magnetic fields from 0 to 1.53 T. The field was varied in a conventional electromagnet with the field perpendicular to both the $\gamma$-ray beam and the *c*-axis of the platelets. Spectra were fitted using a conventional non-linear least-squares minimization routine.

In order to study the reorientation process, a reference frame must first be identified. In a powder sample, the electric field gradient serves as a crystallographic reference frame. The high point symmetries of the three Sn sites in $RMn_6Sn_6$ (6*mm* for Sn−2*e* and $\bar{6}m2$ for Sn−2*c* and Sn−2*d*) cause the crystallographic and electric field gradient axes to coincide, guaranteeing that the principal axis of the electric field gradient tensor $V_{zz}$ lies along *a*, *b* or *c*. The local hexagonal point symmetries also impose axial symmetry ($\eta = 0$), such that the quadrupole splitting $\Delta$ is:

$$\Delta = \frac{eQV_{zz}}{4}(3\,cos^2\theta - 1) \tag{1}$$

where $\theta$ is the angle between $V_{zz}$ and the hyperfine field at the Sn site due to the surrounding magnetic moments. For $\theta = 90°$, $\Delta = -\frac{1}{4}eQV_{zz}$ and for $\theta = 0°$, $\Delta = \frac{1}{2}eQV_{zz}$, so that a change in $\Delta$ by a factor of −2 corresponds to a change in moment direction by 90°.

The intensity of the second and fifth Mössbauer lines depends on the orientation of the magnetic moments with respect to the $\gamma$-ray ($\vartheta$). Writing the intensity ratio as 3:*R*:1:1:*R*:3 for a six line Mössbauer pattern (for a $\frac{3}{2} \rightarrow \frac{1}{2}$ transition, such as in $^{119}Sn$ Mössbauer spectroscopy), $\vartheta$ can be determined:

$$R = \frac{4sin^2\vartheta}{1 + cos^2\vartheta} \tag{2}$$

For a single crystal, the moments point along a well defined direction with respect to the $\gamma$-direction. For example, the $TbMn_6Sn_{5.46}In_{0.54}$ single crystal platelets are grown

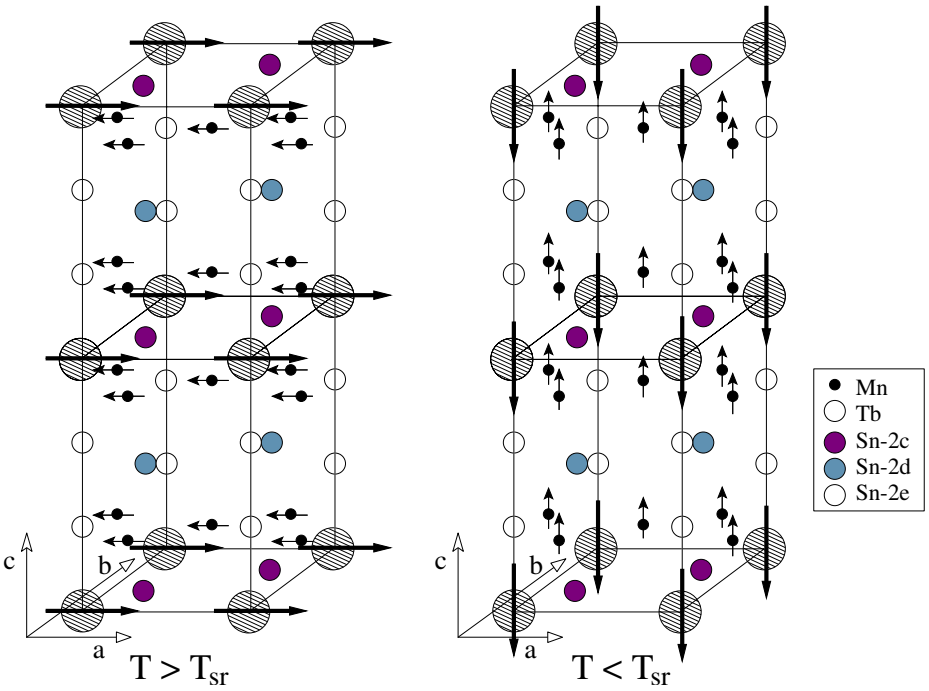


**Figure 1** Crystal and magnetic structure of $TbMn_6Sn_6$ for temperatures above (*left*) and below (*right*) the reorientation temperature, $T_{sr}$.

with $c$ perpendicular to the plane of the plates, parallel to $\gamma$. If the moments lie along the $c$-axis, then $\gamma \parallel c \parallel \mu$, giving $\vartheta = 0°$ and $R = 0$. If the moments are in the $ab$-plane, then $\gamma \parallel c \perp \mu$, giving $\vartheta = 90°$ and $R = 4$. For an oriented sample, $R$ can be used to determine the moment direction. For a powdered sample, $R$ averages to 2 and this information is lost.

## 3 Results

### 3.1 Temperature-induced spin reorientation in $TbMn_6Sn_{6-x}Ga_x$

The $TbMn_6Sn_6$ system has a $HfFe_6Ge_6$-type, $P6/mmm$ crystal structure, with lattice parameters $a = 5.53$ Å and $c = 9.023$ Å [8]. There are three crystallographic Sn sites in this structure: Sn−2$c$ (1/3, 2/3, 0), Sn−2$d$ (1/3, 2/3,1/2) and Sn−2$e$ (0, 0, 0.3356). The Sn−2$c$ and Sn−2$d$ sites both sit in the center of hexagonal $Mn_6$ prisms. Sn−2$c$ is in the plane of three Tb neighbours, while Sn−2$d$ has no rare earth neighbours [5, 8].[1] Sn−2$e$ lies in a hexagonal plane of Mn atoms, with one Tb neighbour above and

[1] In [5], the rare earth atom sits in the Tb−1$a$ site at (0,0,0). Sn−2$c$ has coordinates $(\frac{1}{3},\frac{2}{3},0)$ and so it is in the plane of three Tb atoms. In [8], the rare earth atom sits in the Tb−1$b$ site at $(0,0,\frac{1}{2})$. Thus Sn−2$d$ is labeled as the site in the plane of the rare earths instead of Sn−2$c$.

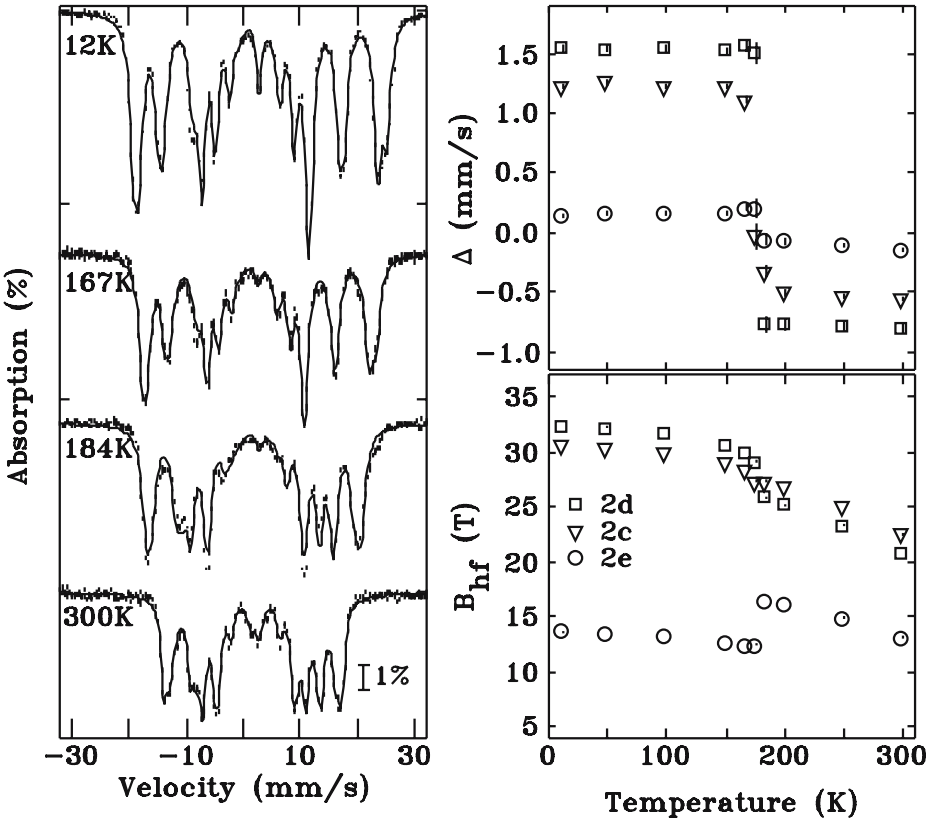


**Figure 2** *Left*: $^{119}$Sn Mössbauer spectra of $TbMn_6Sn_{5.4}Ga_{0.6}$ from 12 to 300 K. *Right*: quadrupole splitting (*top*) and hyperfine field (*bottom*) at the three Sn sites in $TbMn_6Sn_{5.4}Ga_{0.6}$, as functions of temperature. The spin reorientation temperature ($T_{sr}$) is 180(5) K.

one Sn neighbour below. Below $T_N$ = 423 K, the magnetic structure of $TbMn_6Sn_6$ is characterized by alternating ferromagnetic Mn and Tb layers, ordered in the *ab*-plane and stacked along *c* [4] (Figure 1, left). The structure is ferrimagnetic due to strong antiferromagnetic coupling between the Mn and Tb layers. Cooling through $T_{sr} = 330$ K [4] causes the moments to spontaneously reorient onto the *c*-axis (Figure 1, right). The spin reorientation temperature ($T_{sr}$) is a strong function of Ga content ($x$), falling at $255 \pm 18$ K/Ga for increasing $x$ [5].

Figure 2 (left) shows the Mössbauer spectra of $TbMn_6Sn_{5.4}Ga_{0.6}$ from 12 to 300 K. They consist of three subspectra (one for each Sn site) and a central Sn impurity. The assignment of each subspectrum to a Sn site cannot be based on the magnetic neighbours of the Sn sites. As shown in Figure 2 (bottom, right), two of the hyperfine fields (Sn−2*c* and Sn−2*d*) exchange sequence at the reorientation. For instance, if the largest field were to be associated with the site having the most magnetic neighbours, the site assignment would be different depending on whether the measurement were made above or below $T_{sr}$. Instead, the site assignment in [5] was based on the electrostatic environment (quadrupole splitting). This choice is not affected by their

**Table I** Mössbauer parameters at 167 and 200 K in $TbMn_6Sn_{5.4}Ga_{0.6}$

| | $T < T_{sr}$ ($\mu \parallel c$) 167 K | | $T > T_{sr}$ ($\mu \perp c$) 200 K | |
|---|---|---|---|---|
| Site | $\Delta$ (mm/s) | $B_{hf}$ (T) | $\Delta$ (mm/s) | $B_{hf}$ (T) |
| Sn−2*c* | 1.11(3) | 28.40(3) | −0.51(3) | 26.73(3) |
| Sn−2*d* | 1.56(4) | 29.91(4) | −0.77(5) | 25.18(5) |
| Sn−2*e* | 0.21(3) | 12.39(3) | −0.07(3) | 16.20(2) |

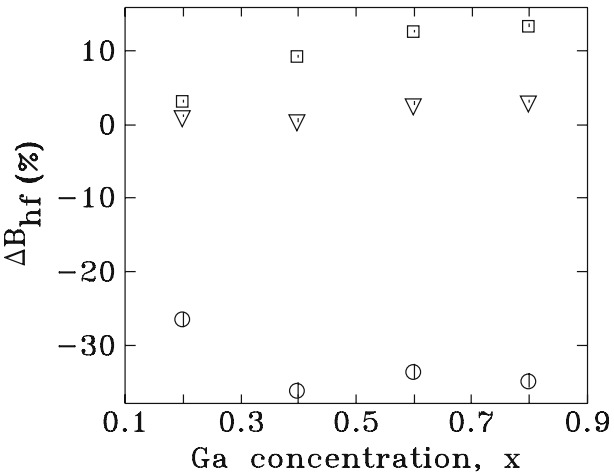


**Figure 3** Fractional change in hyperfine field extrapolated to 0 K on two Brillouin curves, for $T < T_{sr}$ and $T > T_{sr}$.

orientation since the projection of the electric field gradient tensor changes by the same factor for all sites when the moments rotate. Table I lists the parameters for $T < T_{sr}$ and $T > T_{sr}$, where we see that the quadrupole splitting changes by a factor of −2 on cooling through $T_{sr}$ = 180(5) K (Figure 2, top right). This corresponds to a change in moment direction of 90° (as discussed in Section 2), from the *ab*-plane for $T > T_{sr}$ to the *c*-axis for $T < T_{sr}$. The width of the transition is less than 5 K, so the reorientation is an abrupt, well-defined transition.

The temperature dependence of the hyperfine fields at the three Sn sites is shown in Figure 2 (bottom right). On cooling through $T_{sr}$, $B_{hf}$ increases at Sn−2*d* and decreases at Sn−2*e*, and both are dramatic effects. In contrast, the hyperfine field at Sn−2*c* increases only slightly through the reorientation. The temperature dependence of $B_{hf}$ was fitted to two Brillouin functions: one for $T < T_{sr}$ and another for $T > T_{sr}$. The two Brillouin curves were extrapolated to 0 K, and the difference $\delta B_{hf}$ was normalized to the 0 K $B_{hf}$ with $\mu \parallel c$. This gives the fractional change in hyperfine field, $\Delta B_{hf}$, plotted in Figure 3 as a function of composition (Ga content, *x*). The fractional change in $B_{hf}$ differs significantly for each site, and there is evidence for a slight increase in $|\Delta B_{hf}|$ for increasing Ga content.

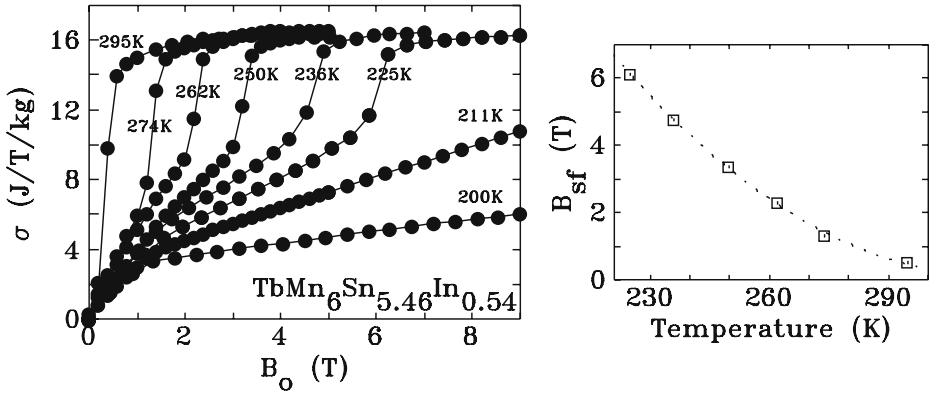


**Figure 4** *Left*: Magnetization of $TbMn_6Sn_{5.46}In_{0.54}$ in an applied field range of 0 to 9 T and for $T < T_{sr}$. The applied field is perpendicular to the *c*-axis. *Right*: Temperature dependence of the spin-flop field in $TbMn_6Sn_{5.46}In_{0.54}$ for $T < T_{sr}$. The *dotted line* is a guide to the eye.

## 3.2 Field-induced spin-flop in $TbMn_6Sn_{5.46}In_{0.54}$

### *3.2.1 Magnetometry*

The thermal variation of the magnetization of the single crystals measured above room temperature indicates the Néel point to be $T_N$= 397 K for $TbMn_6Sn_{5.46}In_{0.54}$. In addition, the compound displays a spin reorientation transition at $T_{sr}$ = 317 K characterized by a change of the easy direction from the *ab*-plane at high temperature ($T > T_{sr}$) to the *c*-axis for $T < T_{sr}$.

Figure 4 (left) shows the magnetization of a $TbMn_6Sn_{5.46}In_{0.54}$ single crystal as a function of applied field, where $B_o$ is perpendicular to *c*, and $T < T_{sr}$. In an applied field of ∼0.5 T at room temperature, a spin-flop is induced to the direction along which $B_o$ is applied (*ab*-plane). This confirms the moments are along the *c*-axis at room temperature. The spin-flop field increases with decreasing temperature (Figure 4, right). As the spin-flop field is expected to exceed the available 9 T at 220 K, the spin-flop is unattainable for 211 K and below.

### *3.2.2 Mössbauer spectroscopy*

Figure 5 (left) shows the Mössbauer spectra for $TbMn_6Sn_{5.46}In_{0.54}$ in applied fields ranging from 0 to 1.53 T. In order to assign the subspectra to Sn sites as seen in Section 3.1, the sample was cooled to 12 K where the Mössbauer lines are more distinguishable. The site assignments at 12 K followed those of the $TbMn_6Sn_{6-x}Ga_x$ case [5] and sample parameters are shown in Table II. At 300 K, the quadrupole splittings were set to those determined at 12 K and the fields and isomer shifts were adjusted freely. The area constraint was 1:1:1.

For the single crystal platelets of $TbMn_6Sn_{5.46}In_{0.54}$, the moments are oriented along a unique direction with respect to the $\gamma$ propagation direction. Through magnetometry it was shown that at 295 K and below, the moments are along the *c*-axis (parallel to $\gamma$). The intensity ratio *R* is plotted in Figure 5 (top right) as a function of applied field.

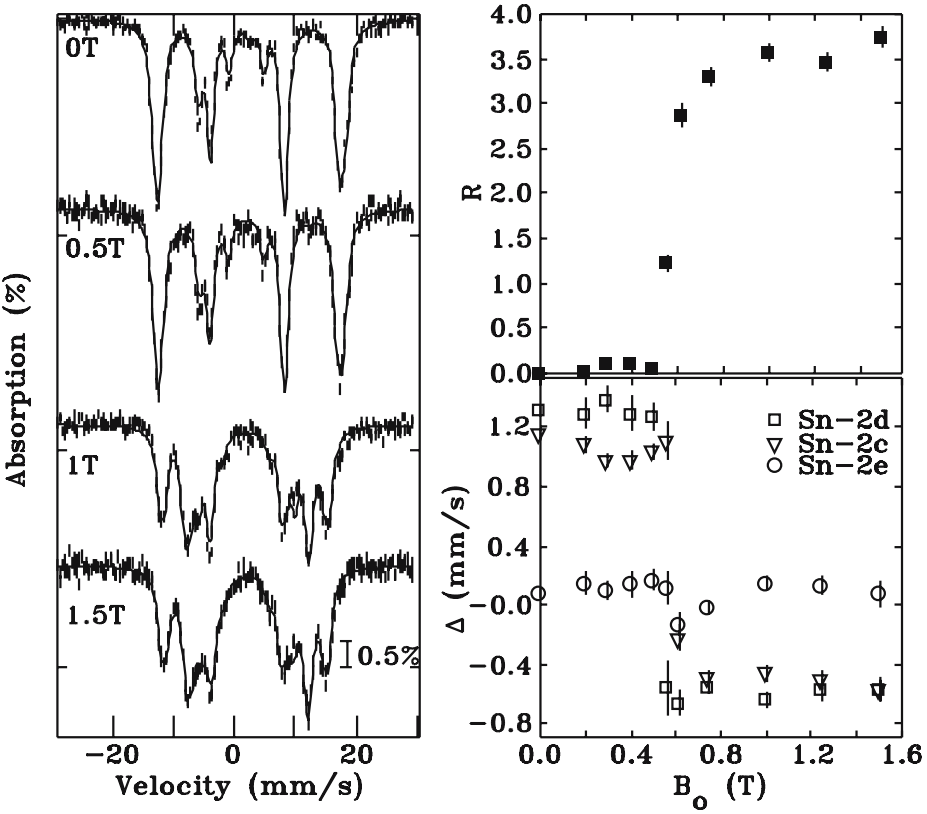


**Figure 5** *Left*: $^{119}$Sn Mössbauer spectra of $TbMn_6Sn_{5.4}Ga_{0.6}$ from 0 to 1.53 T. *Right*: *R* ratio (*top*) and quadrupole splitting (*bottom*) of the three Sn sites as functions of applied field. The spin-flop occurs at $B_{sf}$ =0.57(3) T.

**Table II** Mössbauer parameters at 12 K in $TbMn_6Sn_{5.4}Ga_{0.6}$ and $TbMn_6Sn_{5.46}In_{0.54}$. The comparison of parameters between the two similar compounds guided the site assignment in $TbMn_6Sn_{5.46}In_{0.54}$

| T = 12 K | $TbMn_6Sn_{5.4}Ga_{0.6}$ ($\mu \parallel c$) | | $TbMn_6Sn_{5.46}In_{0.54}$($\mu \parallel c$) | |
|---|---|---|---|---|
| Site | Δ (mm/s) | $B_{hf}$ (T) | Δ (mm/s) | $B_{hf}$ (T) |
| Sn−2*c* | 1.23(2) | 30.57(2) | 1.09(5) | 26.26(2) |
| Sn−2*d* | 1.55(3) | 32.39(3) | 1.33(9) | 27.94(3) |
| Sn−2*e* | 0.14(2) | 13.64(2) | 0.02(4) | 12.23(2) |

For $B_o < B_{sf}$, $R = 0$ confirms that the moments are parallel to the $\gamma$-rays ($\vartheta = 0°$) and thus to *c*. Once the spin-flop has occurred, an abrupt change in *R* from 0 to 3.7(1) is observed, indicating a change in moment direction. *R* is not 4 as expected for a full rotation into the *ab*-plane. This could either be due to an incomplete

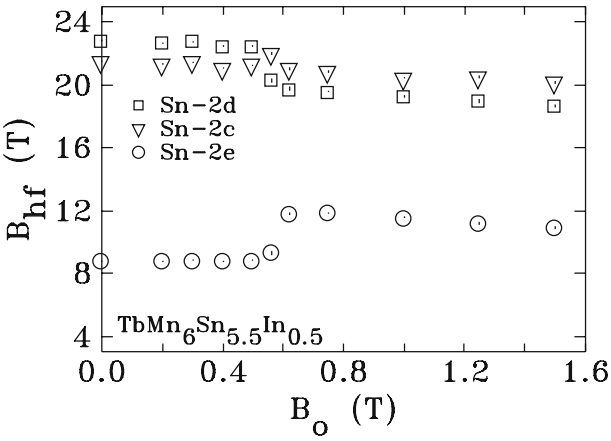


**Figure 6** Hyperfine fields at the three Sn sites in $TbMn_6Sn_{5.46}In_{0.54}$. The reorientation of the moments at 0.57(3) T on increasing applied fields causes an increase in $B_{hf}$ at Sn−2*e*, and a decrease in $B_{hf}$ at Sn−2*c* and Sn−2*d*.

**Table III** In $TbMn_6Sn_{5.4}Ga_{0.6}$, the two $T < T_{sr}$ and $T > T_{sr}$ Brillouin curves are extrapolated to T = 0 K. The difference $\delta B_{hf}$ is normalized to the 0 K $B_{hf}$ with $\mu \parallel c$ to give the fractional change $\Delta B_{hf}$. In $TbMn_6Sn_{5.46}In_{0.54}$, the two $B_o < B_{sr}$ and $B_o > B_{sr}$ lines of slope −1 are extrapolated to 0 T. The difference $\delta B_{hf}$ is normalized to the 0 T $B_{hf}$ with $\mu \parallel c$, giving $\Delta B_{hf}$

| | $TbMn_6Sn_{5.4}Ga_{0.6}$ T-induced | | $TbMn_6Sn_{5.46}In_{0.54}$ $B_o$-induced | |
|---|---|---|---|---|
| Site | $\delta B_{hf}$ (T) | $\Delta B_{hf}$ (%) | $\delta B_{hf}$ (T) | $\Delta B_{hf}$ (%) |
| Sn−2*c* | 0.6(2) | 2.6(5) | 0.02(2) | 0.9(9) |
| Sn−2*d* | 3.9(2) | 12.7(4) | 2.38(4) | 10.4(2) |
| Sn−2*e* | −4.9(1) | −34(2) | −4.1(1) | −45(3) |

rotation of the moments or to saturation effects. However, the factor of −2 change in quadrupole splitting (Figure 5, bottom right) associated with the spin-flop confirms that the rotation is complete. Therefore, the effect is likely due to the saturation of lines 2 and 5, caused by samples which are somewhat thick (the platelet thickness is ∼60 $\mu$m).

Figure 6 shows the hyperfine fields at the three Sn sites as functions of applied field. For increasing $B_o$, the spin-flop is associated with an increase in $B_{hf}$ at Sn−2*e*, and a decrease at Sn−2*c* and Sn−2*d*. These effects are identical to those observed in the thermally-driven spin reorientation in $TbMn_6Sn_{6-x}Ga_x$.The field dependence of $B_{hf}$ was fitted to two lines of slope −1: one for $B_o < B_{sf}$ and another for $B_o > B_{sf}$. The lines were extrapolated to 0 T, and the difference $\delta B_{hf}$ was normalized to the 0 T $B_{hf}$ with $\mu \parallel c$ to give the fractional change in hyperfine field, $\Delta B_{hf}$. In Table III, $\Delta B_{hf}$ is compared to that obtained in the thermally-driven reorientation in $TbMn_6Sn_{5.4}Ga_{0.6}$. The close agreement between the two measurements of $\Delta B_{hf}$ demonstrates that the anisotropic contribution can be obtained through both temperature-induced and field-induced spin reorientation and that it is independent of the driving force. The fractional change in hyperfine field due to the anisotropic contribution is large and negative in the case of Sn−2*e*, and smaller and positive at the Sn−2*c* and Sn−2*d* sites.

**Table IV** Vector sum over the six Mn neighbours ($\mathbf{A}_1$) for the three Sn sites in applied fields $B_o < B_{sf}$ and $B_o > B_{sf}$. The arrows in the third column indicate the magnitude $A_1/A_p$

| | $\mathbf{A}_1/A_p$ | | |
|---|---|---|---|
| Site | $B_o < B_{sf}$ $\mu \parallel c$ | $B_o > B_{sf}$ $\mu = (\frac{1}{\sqrt{2}}, \frac{1}{\sqrt{2}}, 0)\ \mu$ | $\Delta A_1/A_p$ |
| Sn−2*c* | $(0, 0, 3.97\mu)$ | $(0.72\mu, 0.72\mu, 0) \rightarrow 1.01\ \mu$ | $2.96\ \mu$ |
| Sn−2*d* | $(0, 0, 4.02\mu)$ | $(0.70\mu, 0.70\mu, 0) \rightarrow 0.99\mu$ | $3.03\ \mu$ |
| Sn−2*e* | $(0, 0, 0.46\mu)$ | $(1.96\mu, 1.96\mu, 0) \rightarrow 2.77\mu$ | $-2.31\ \mu$ |

Since the isotropic contribution to $B_{hf}$ is independent of moment orientation, the changes in $B_{hf}$ due to the spin-flop directly relate to the anisotropic contribution. The hyperfine field transferred to the Sn sites is given by [2, 3]:

$$\mathbf{B}_{hf} = \left( A_p \sum_{i=1}^{6} \mathbf{u}_i(\mu_i \cdot \mathbf{u}_i) - \frac{A_p}{3} \sum_{i=1}^{6} \mu_i \right) + A_s \sum_{i=1}^{6} \mu_i \tag{3}$$

where $\mathbf{u}_i$ is the unit vector connecting each Sn atom to a specific Mn atom with moment $\mu_i$. $A_p$ and $A_s$ are the dipolar and contact fields due to a unit Mn moment. $A_p$ is also referred to as the anisotropic constant. The last term in Eq. 3 is the isotropic contribution from the Mn shells around the Sn atoms, while the first two terms represent the anisotropic part of the transferred hyperfine field. For the spin-flop, we will only consider the first term ($\mathbf{A}_1$) of Eq. 3 involving the dot product, because the second term is independent of moment direction. The dot product $(\mu_i \cdot \mathbf{u}_i)$ is a maximum when the moment and Mn–Sn bond are parallel, and zero when they are perpendicular. From the crystal structure we know that the Mn–Sn bonds make angles of 35° (Sn−2*c* and Sn−2*d*) and 73° (Sn−2*e*) with the *c*-axis. From the Mössbauer results discussed above (and from magnetometry and neutron scattering [9]), at $T < T_{sr}$ we know that the moments point along *c* for $B_o < B_{sf}$ and in the *ab*-plane for $B_o > B_{sf}$. As all the angles and orientations are known for any $B_o$, the anisotropic constant $A_p$ can be determined.

Table IV lists the values for $\mathbf{A}_1$ at Sn−2*c*, Sn−2*d* and Sn−2*e* in applied fields above and below the spin-flop field. When the moments flop into the *ab*-plane from the *c*-axis, $A_1$ decreases at Sn−2*c* and Sn−2*d*, while it increases at Sn−2*e*. Comparisons between $\Delta A_1/A_p$ and $\Delta B_{hf}$ show that despite their relative magnitudes being inconsistent, the signs of both quantities agree for all three Sn sites. The sign of $\Delta A_1/A_p$ for each Sn site mirrors the behaviour of the overall transferred hyperfine fields of Figure 6 and Table III, indicating that the anisotropic and isotropic contributions have the same sign. The Sn−2*e* site was previously assigned by elimination in $TbMn_6Sn_{6-x}Ga_x$ [5]: Sn−2*c* was assigned to the subspectrum which most reflected the values seen in $HfMn_6Sn_6$ [1], the Sn−2*d* site assignment was argued based on similarity to Sn−2*c*, and the remaining subspectrum was assigned Sn−2*e*. Here we see that Sn−2*e* is unique because it has a negative $\Delta A_1/A_p$ and $\Delta B_{hf}$. This distinction allows the Sn−2*e* site to be directly identified and confirms that the site assignment in $TbMn_6Sn_{6-x}Ga_x$ was correct.

In the tetragonal $MnSn_2$ system (*I*4/*mcm*, *a* = 6.659 Å, *c* =5.447 Å, with Mn−4*a* at (0, 0, 0.25) and Sn−8*h* at (0.1623,0.6623, 0)), there is no spin reorientation or

**Table V** Calculated anisotropic contributions to $B_{hf}$ at the three Sn sites in $TbMn_6Sn_{5.46}In_{0.54}$. The anisotropic field $B_{hf}^A$ is equal to $\delta B_{hf}$ from Table III

| Site | $\Delta A_1/A_p$ ($\mu$) | $B_{hf}^A$ (T) | $A_p$ (T/$\mu_B$) |
|---|---|---|---|
| Sn−2*c* | 2.96 | 0.02(2) | 0.003(2) |
| Sn−2*d* | 3.03 | 2.38(4) | 0.39(2) |
| Sn−2*e* | −2.31 | −4.1(1) | 0.89(5) |

spin-flop, and $\Delta A_1$ is simply $A_1$. The size of $A_1/A_p$ is 0.96 $\mu$ and the magnitude of the Mn moment is $\mu$ = 2.33 $\mu_B$ [2]. The antiferromagnetic environment of the $Sn_{00}$ site guarantees that the transferred hyperfine field at $Sn_{00}$ is purely anisotropic. The anisotropic transferred hyperfine field $B_{hf}^A$ relates to the anisotropic constant $A_p$ through:

$$A_p = \frac{B_{hf}^A}{\Delta A_1} \tag{4}$$

At $Sn_{00}$, $B_{hf}^A$ = 4.9(2) T, giving the anisotropic constant $A_p$ = 2.19(1) T/$\mu_B$ [2]. For the spin-flop in $TbMn_6Sn_{5.46}In_{0.54}$, the anisotropic field $B_{hf}^A$ is taken as the difference between the $\mu \parallel c$ and $\mu \perp c$ hyperfine fields extrapolated to $B_o$ = 0 T ($\delta B_{hf}$ from Table III). From room temperature neutron diffraction studies of $TbMn_6Sn_6$, we know that the Mn moment is 1.99(6) $\mu_B$ [9]. The anisotropic constant $A_p$ in $TbMn_6Sn_{5.46}In_{0.54}$ can therefore be determined for all three Sn sites (Table V).

The anisotropic constants at the Sn sites in $TbMn_6Sn_{5.46}In_{0.54}$ are significantly smaller than $A_p$ measured at the $Sn_{00}$ site in $MnSn_2$ (which is the only site allowing for the cancellation of the isotropic contribution). As the anisotropic contribution is related to the localization of electrons on the Mn–Sn bond, and therefore to covalency effects [2], the smaller anisotropic constants seen here could suggest that the Mn–Sn bonds in $TbMn_6Sn_{5.46}In_{0.54}$ are less covalent. Parasitic anisotropic effects arising from Tb–Sn bonding could also reduce the Mn–Sn anisotropic contribution in this system, leading to smaller anisotropic constants.

## 4 Conclusions

The Mössbauer study of the temperature-induced spin reorientation and the field-induced spin-flop (in $TbMn_6Sn_{6-x}Ga_x$ and $TbMn_6Sn_{5.46}In_{0.54}$ respectively) has demonstrated that the anisotropic contribution to the transferred hyperfine field is independent of the force which drives the reorientation. We have used magnetometry and Mössbauer spectroscopy to show that the moments are along the *c*-axis for $T < T_{sr}$. The change in anisotropic field at the reorientation is seen to be largest at the Sn−2*e* site, and the identification of this site is validated. The anisotropic contribution has been shown to be substantial, though less than in the $MnSn_2$ system, a possible consequence of weaker covalent bonding or contributions from Tb–Sn bonds. Future investigations of non-magnetic rare earth compounds will be performed with the intent of evaluating the possibility of a parasitic anisotropic effect from R–Sn (R = magnetic rare earth) bonding. The replacement of magnetic

Tb with a non-magnetic rare earth atom also allows for further studies of covalency effects in the $RMn_6Sn_6$ system.

## References

1. Mazed, T., Tobola, J., Venturini, G., Malaman, B.: Phys. Rev., B **65**, 104406 (2002)
2. Le Caër, G., Malaman, B., Venturini, G., Kim, I.B.: Phys. Rev., B **26**, 5085 (1982)
3. Le Caër, G., Malaman, B., Venturini, G., Fruchart, D., Roques, B.: J. Phys. F. Met. Phys. **15**, 1813 (1985)
4. Venturini, G., Chafik El Idrissi, B., Malaman, B.: J. Magn. Magn. Mater. **94**, 35 (1991)
5. Perry, L.K., Ryan, D.H., Venturini, G., Cadogan, J.: J. Appl. Phys. **99**, (2006)
6. Lefèvre, C., Venturini, G., Malaman, B.: J. Alloys Compd. **346**, 84 (2002)
7. Clatterbuck, D.M., Gschneidner, K.A. Jr.: J. Magn. Magn. Mater. **207**, 78 (1999)
8. Chafik El Idrissi, B., Venturini, G., Malaman, B.: Mater. Res. Bull. **26**, 431 (1991)
9. Chafik El Idrissi, B., Venturini, G., Malaman, B.: J. Less-common Met. **175**, 143 (1991)